MAXIMUM RIPPLE ELIMINATING MULTI-LEVEL BIDIRECTIONAL DC-DC CONVERTER VIA OPTIMIZED DEEP LEARNING NETWORK

JAWAHAR MARIMUTHU[1], EDWARD RAJAN[1]

Keywords: Personal mobility devices; Deep learning; Charging stations; Modified emperor penguin optimization; Duty cycle.

In this research, a novel deep learning based Multi-level Bidirectional DC-DC converter using a modified Emperor Penguin Optimized multi-graph neural network (MEPO-MGN[2]) has been proposed. Grid power is converted to direct current by means of an AC-DC converter, and then a bidirectional multi-level DC-DC converter (MLDC) is used for the power transfer in both directions between the grid and PMDs. The proposed method utilizes an attention multi-graph convolution network (AMGCN) for the duty cycle (α) prediction of MLDC to regulate the flow of power between the grid and PMD, vice versa. This system employs multiple Proportional-Integral (PI) controllers to manage voltage and current for stable, optimized power transfer. Modified emperor penguin optimization (MEPO) is used to tune the parameters of MLDC, thereby achieving a well-regulated DC output voltage in the charging stations. The MEPO-MGN[2] performance is evaluated, and implementation is carried out using the MATLAB platform. The efficacy of the proposed method is 98.5%, which is better than the other existing converter techniques.

1. INTRODUCTION

Over the recent years, the evolution of transportation electrification has received considerable attention from nations worldwide [1]. Electric vehicles (EVs) are considered the objective of reaching zero carbon emissions as an alternative to achieving carbon neutrality. Globally, electric mobility, or E-Mobility, has accelerated the decarbonization of transportation. Electric vehicles (EVs) may replace gasoline-powered automobiles with the use of lithium-ion batteries (LIBs) [2]. Electric-powered vehicles that require a charger or other infrastructure to recharge their batteries are referred to as "e-mobility" [3].

Sustaining a low battery rated voltage is beneficial to vehicle performance since it allows for the use of fewer cells linked in series [4]. Conventional converters used in EVs often face challenges such as limited voltage gain and high switching losses [5]. Charging stations are advanced infrastructures designed to quickly charge PMDs, which allow users to recharge their devices [6]. Charging stations for PMDs show a critical role in enabling the prevalent adoption of these devices, as users need to be able to charge their devices conveniently and reliably [7]. Therefore, a novel topology for charging and a switching mechanism that can use it are necessary with the purpose of fulfilling the charging current's ripple rate, irrespective of the necessary charging current across all chargeable voltage zones, varying from 12 V to 60 V [8]. Multilevel converters have appeared as an optimistic result to overcome these difficulties, presenting advantages like decreased voltage stress on components, improved efficiency, and scalability for high-power applications [9,10]. In this research, an MLDC converter using a modified Emperor Penguin Optimized multi-graph neural network (MEPO-MGN[2]) is proposed. The significant contribution of the approached method is described as:

- This manuscript proposed a novel method called MEPO-MGN[2] to develop a smart charging station by reducing the charging current ripple and enhancing the efficiency, thereby providing a well-regulated DC output voltage for charging.
- This research utilized an AC-DC converter for the initial conversion of grid power into a stable DC voltage and a multi-level bidirectional converter (MLDC) for the power flow in both directions between PMDs and the grid.

- The proposed method employs an Attention Multi Graph Convolution Network (AMGCN) for the prediction of duty cycle (α) of the MLDC converter, thereby controlling the bidirectional power flow capability.
- Modified emperor penguin optimization (MEPO) is used for tuning the parameters of the MLDC converters by optimizing the duty ratio and switching frequency of the MLDC converter.

The structure of the study is given as follows: Section 2 explains the related works on E-mobility. Section 3 presents the proposed multilayer charging mechanism. The findings and the MLDC operation experiment are then described in Section 4. Conclusion and future work are provided in Section 5.

2. LITERATURE SURVEY

A diode-parallel multilevel converter, which consists of an independent Buck converter connected in series, was introduced by Lee, J.H. et al. [11] in 2020. The switch on the buck converter is placed at the negative terminal of the input power source so that the supply voltage can be used as the gate amplifier voltage. A DC transformer topology based on a modular multilevel converter (MMC) and cascaded H-bridge was proposed by Sha, G. et al. [12] in 2021. The evidence is consistent with the theoretical analysis.

In 2021, Han, X., and Wen, H. [13] designed a modular multi-level DC transformer (MMDC) that produces dual active bridge (DAB) and modular multi-level converter (MMC). The gate signals from higher to lower voltages in capacitors. The simulation results show that the capacitor voltage changes. In 2022, Sarkar, S., and Das, A. [14] proposed a DC–DC modular multilevel converter (MMC) that enables numerous EVs to be charged quickly. The suggested converter is verified using a scaled-down lab prototype and simulation model. A multilayer bridge tapped resonant (MBTR) converter for battery-to-grid integration was proposed in 2023 by Dube, S.K. et al. [15]. An efficiency of 95.8% is achieved with a switching frequency of 85–95 kHz.

A topology equivalent circuit design of a three-level pulse width modulation rectifier was presented by Huang, Y., et al. [16] in 2023. Because of their notable performance benefits, the three-level AC/DC and three-level bidirectional DC/DC converters used in this study offer genuine assistance for the EV charging station. A SOC-Based Fast and Stable Charging

[1] Mepco Schlenk Engineering College (Autonomous), Sivakasi, Tamil Nadu, India.
E-mails: jawahar.m@mepcoeng.ac.in (correspondence), sedward@mepcoeng.ac.in

Control for EVs using a Multilevel DC-DC Buck Converter was presented in 2024 by Ray, K.B., and Kumar, R. [17]. To show the appropriateness of the suggested billing system, a comparison study is performed.

In 2025, Jothimani, G. et al. [18] proposed a high-gain DC-DC converter with a lower part count for light electric vehicle (LEV) applications. Furthermore, MATLAB/Simulink is utilized to simulate the proposed configuration, which confirms the theoretical findings, and a 100 W laboratory prototype of the same is fabricated and tested to verify the performance of the presented converter. In 2025, Duraisamy, M. [19] suggested an integrated non-isolated DC-DC power converter construction that combines voltage-gain-boosted Cuk topologies with conventional SEPIC (single-ended primary inductor converter) in tandem. An experimental setup is created, and its outcomes are compared with those of the MATLAB/Simulink topology model in order to verify the efficacy of the suggested integrated converter structure.

Compared with recent state-of-the-art multilevel DC–DC charging systems, which mainly focus on hardware topology and fixed control strategies such as MMC-DAB structures [12,13], isolated bidirectional converters [14], and SOC-based buck converters [17], the proposed HSWO–AMGCN-based MLDC framework is technically superior because it introduces intelligent, system-level energy management rather than only component-level regulation. While existing methods regulate voltage, gain, or SoC using PI or rule-based controllers and treat each EV or PMD independently, they cannot capture spatial coupling, shared DC-link dynamics, or multi-charger interactions in fast-charging stations. In contrast, the proposed attention-based multi-graph convolution network (AMGCN) explicitly models the electrical and operational interdependence between multiple PMDs, MLDC stages, and the DC bus, enabling coordinated power allocation and ripple-aware control. In the proposed system, modified emperor penguin optimization (MEPO) is used as a global optimizer to automatically determine the best operating parameters for the converter and the intelligent controller.

3. PROPOSED MEPO-MGN^2 METHODOLOGY

In this study, a multi-level bidirectional DC-DC (MLDC) converter using a modified Emperor Penguin Optimized multi-graph neural network (MEPO-MGN^2) has been proposed. Power from the grid is fed to the AC-DC converter for conversion and to regulate the bidirectional power flow, the DC voltage is fed to the MLDC converter (Fig 1).
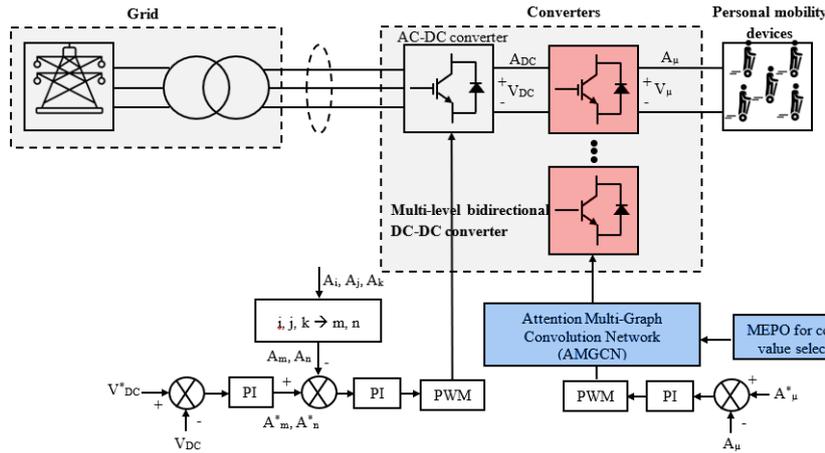

Fig. 1 – Architecture of the proposed MEPO-MGN^2.

3.1. MULTILEVEL DC-DC CONVERTER (MLDC)

MLDC is utilized in the proposed smart charging system for PMDs. Multi-level topologies are typically employed to overcome the switching elements' voltage restriction in order to handle high-voltage converters. The current ripple γx_L of the inductor is expressed as,

$$\gamma x_L = \frac{U_s}{L} V_x g(1-g), \qquad (1)$$

U_s is the Switching period of the converter, and the output voltage ripple γV_{out} is expressed as,

$$\gamma V_{out} = \frac{V_x g(1-g)U_s^2}{8Lg}, \qquad (2)$$

where V_x, L and g are determined by the design conditions of buck boost convertor. The duty ratio alone determines the inductor's current and output voltage ripple while regulating the converter. The input voltage of the MLDC is made up of V_x/P_{total}, which we defined as V_{xst} in this study, in contrast to the input voltage V_x. To generate the output voltage V_{out}, the MLDC uses V_{xst} the input to determine the number of levels P_{stg}. The duty ratio g_{st} of the output voltages V_{out} P_{stg} can be written as follows:

$$V_{out} = V_{xst}\big(P_{st} + (g_{st} - 1)P_{stg}\big), \qquad (3)$$

$$g_{st} = V_{out} - \left(\frac{V_{xst} \times (P_{st} - P_{stg})}{V_{xst} \times P_{stg}}\right). \qquad (4)$$

P_{stg} is the number of active converter stages contributing to the output voltage If the number of converters V_{xst}. Then, the current ripple and output voltage ripple of the inductor can be expressed as

$$\gamma x_L = \frac{U_s}{L} V_{xst} g_{st}(1-g_{st}), \qquad (5)$$

$$\gamma V_{out} = \frac{V_x g_{st}(1-g_{st})U_s^2}{8Lg}. \qquad (6)$$

However, if $P_{stg} > 1$, then the current is enclosed by P_{stg}, causing a reduction in the current ripple γx_L. The current ripple cancellation effect Cr_l can be written as

$$Cr_l = \frac{P_{stg}\left(g_{st} - \frac{m}{P_{stg}}\right)\left(\frac{m+1}{P_{stg}} - g_{st}\right)}{g_{st}(1-g_{st})}, \qquad (7)$$

$$\gamma x_L = \frac{Cr_l}{L} V_{xst} g_{st}(1-g_{st}). \qquad (8)$$

The output voltage ripple of the MLDC γV_{out} is given as follows:

$$\gamma V_{out} = \frac{V_x g_{st}(1-g_{st})U_s^2}{8Lg \times P_{stg}}. \qquad (9)$$

The inverter is not included in the number of inverters using PWM if its exchanging condition is active. The multilevel bidirectional DC–DC converter (MLDC) interfaces the grid-side DC link and the PMD battery. It receives the switching signals from the PWM generator and produces the electrical outputs.

3.2 BIDIRECTIONAL POWER FLOW CONTROL USING AMGCN

Bi-directional power flow of MLDC converter is regulated using an attention multi-graph convolution network (AMGCN) to address voltage unbalance issues and keep the charging current ripple at a low level. The Attention multi-graph convolution network (AMGCN) acts as an adaptive nonlinear controller. Specifically, AMGCN is used as a controller to determine the output current and voltage of the MLDC converter. Figure 2 depicts the architecture of AMGCN.
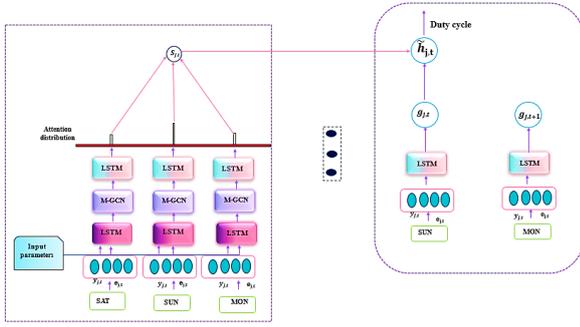

Fig. 2 – Architecture of AMGCN.

AMGCN is used for functions that involve structured data with multiple graphs. AMGCNs use multiple graph convolutional layers to extract features from each graph independently, and then combine them to make a final prediction of switching states. Here, to simulate the spatial and temporal relations, a "hamburger" structure comprising two LSTMs and a single multi-graph convolution layer (M-GCN) is used. Finally, spatial-temporal relations are aggregated using a second LSTM. Then the information is passed to the second phase and incorporated with an attention mechanism to generate the predicted output.

An LSTM network is used to describe this local temporal relation because each charging station's flow pattern differs greatly. The memory of the previous time step g_{t-1} and the pertinent data at the present time step x_t are the two inputs that the LSTM receives at each time step t. Three gates—the input gate, output gate, and forget gate control this process. These gates can be expressed as follows:

$$f_{j,t} = \sigma\big(T_f[g_{i,t-1}, x_{j,t}] + b_f\big), \tag{1}$$
$$i_{j,t} = \sigma(T_i[g_{j,t-1}, x_{j,t}] + b_i), \tag{2}$$
$$\widetilde{C_{j,t}} = \tanh\big(T_C[g_{j,t-1}, x_{j,t}] + b_c\big), \tag{3}$$
$$C_{j,t} = f_{j,t} \circ C_{j,t-1} + i \circ \widetilde{C_{J,t}}, \tag{4}$$
$$o_{j,t} = \sigma\big(T_o[g_{j,t-1}, x_{j,t}] + b_o\big), \tag{5}$$
$$g_{i,t} = o_{j,t} \circ \tanh\big(C_{j,t}\big), \tag{6}$$

where $f_{j,t}, i_{j,t}, o_{j,t}$ are the forget, input, and output gate respectively. $\sigma, tanh$ are the non-linear activation functions. T_f, T_i and T_o are the trainable parameters, while b_f, b_i, b_o are the bias vectors of the trainable parameters. Regarding the inputs of step t, the external features $e_{j,t}$ are combined with the flow $y_{j,t}$

$$x_{j,t} = y_{j,t} \oplus e_{j,t}. \tag{7}$$

To model the spatial relations, the multi-graph convolution is proposed and is expressed as

$$G_t = \sigma(\textstyle\sum_{A \in A} \mathbf{A} * \mathbf{H}_t * \mathbf{W}), \tag{8}$$

where $\mathbf{A}$ is the graph set, $\mathbf{H}$ is the feature matrix of all stations, σ is the nonlinear activation function, and $\mathbf{W}$ is a trainable matrix, which will be updated during the training. The predicted duty cycle is sent to the PWM generator, which drives the MLDC switches. MEPO continuously optimizes the neural controller and converter parameters to ensure minimal ripple, fast transient response, and high efficiency.

3.3 PARAMETER TUNING VIA MEPO

In this work, modified emperor penguin optimization (MEPO) is utilized for tuning the hyperparameters of the AMGCN. The MEPO algorithm has been shown to be effective in optimizing the parameters of the DMGNN control system for the MLDC converter. Assume that the wind gradient and velocity is compute as follows.

$$\rho = \perp \alpha, \tag{9}$$
$$R = \alpha + \eta, \tag{10}$$

where α is a random vector and η is an imaginary constant.

To survive the winter, penguins conserve heat in groups. If the polygon radius (R) is greater than 1, the temperature (t) is assumed to be set to 0. Otherwise, temperature (t) is set to 1.

$$E = \left(e - \frac{Max_{iteration}}{z - Max_{iteration}}\right), \tag{11}$$
$$t = \begin{cases} 0, P \geq 1, \\ 1, P \leq 1, \end{cases} \tag{12}$$

where x is the current frequency and t is the temperature profile. All other Imperial Penguin positions will be changed correspondingly.

$$\vec{S} = Dfw\left(F(\vec{U})\vec{X}(w) - C\,\overrightarrow{Dfr}(w)\right) \tag{13}$$

where Y and Z are used to avoid collisions between emperor penguins. The current iteration is Rs. Q represents the top penguin $\vec{S}$, which represents the position of the sovereign penguin. The social power emperor penguins use to find the best solution is called b().

$$\vec{U} = \left(M \times \left(E + X_{grid}(\text{Accuracy})\right) \times \text{Rand}()\right) - E, \tag{14}$$
$$X_{grid}(\text{Accuracy}) = Dfw\left(\vec{X} - \overrightarrow{Xwr}\right), \tag{15}$$
$$\vec{C} = \text{Rand}(\ ). \tag{16}$$

A motion parameter N with a value of 2 is used to isolate penguins. The precision of the polygon grid is expressed as q grid, and the random function Rand () takes values between [0, 1],

$$\overrightarrow{Y(U)} = \sqrt{(hq^{-w}y - q^{-w})^2}. \tag{17}$$

Here, e is an expression characteristic, and g and l are control limits, and their values are in the range [2, 3] and [1.5, 2], respectively.

$$\overrightarrow{Xfr}(W + 1) = \vec{X}(W) - \vec{U}.\vec{S}, \tag{18}$$

where Qep(s+1) is the optimal solution, while repeating this, the penguin changes position.

As a result, MEPO adjusts the MLDC converter's duty ratio and switching frequency to forecast the converter's ideal switching state and reduce current ripple. The suggested model's workflow is shown in Fig. 3.
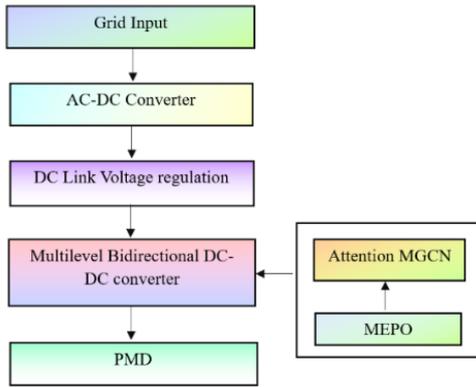
Fig 3. – Control block of the proposed model.

4. RESULT AND DISCUSSION

The simulation results of the MEPO-MGN^2 are presented in this study. MATLAB Simulink is used for the simulation. Details of the reproduction circuit used to test the proposed

staggered MLDC converter are provided in Table 1.

Table 1

Parameters of the proposed simulation circuit.

Parameter	Value
Input DC voltage	12 V
Switching frequency	20 kHz
Load resistance	600 Ω
Inductor	200 µH
Output capacitor	10 µF
Power flow	Bidirectional (charge & discharge)
Simulation platform	MATLAB/Simulink

The output inductor has an inductance value of 200 µH, and the converter's input voltage is set to 12 V. The output capacitor capacitance is 10 µH, and the output load resistance is set to 600 Ω. The switching frequency used in the simulation is 20 kHz. The capabilities of the modeling software and the specifications of the proposed charging system were taken into consideration when choosing these parameters.
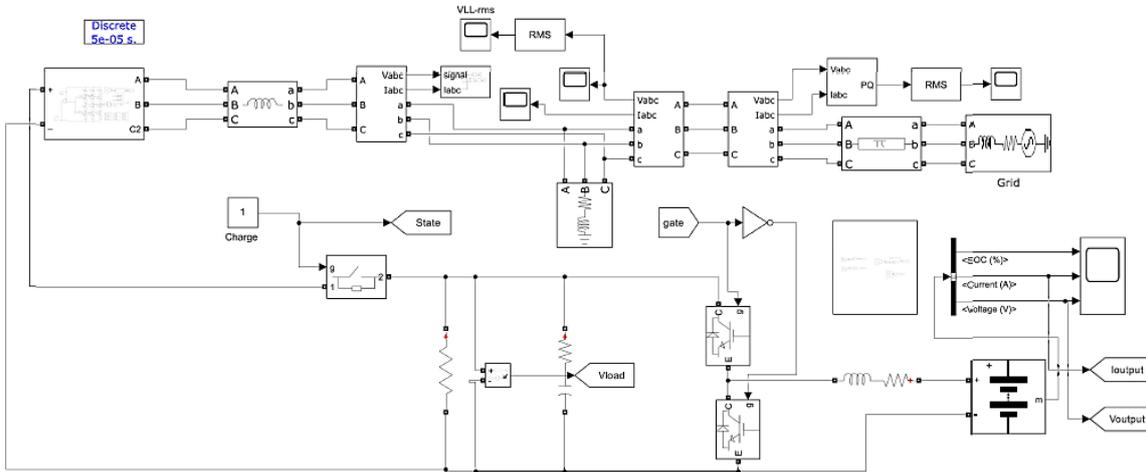

Fig. 4 – Simulation circuit design of the proposed MLDC converter.

Figure 4 represents the Simulation circuit design of the proposed MLDC converter. Three H-bridges are in series connection to comprise the circuit. Two diodes (D1 and D2) and four switches (S1-S4) make up an H-bridge. A pulse width modulation (PWM) signal from a controller powers the switches. The left and right H-bridges are connected to the load and the battery, respectively, while the middle H-bridge is attached to the DC source.
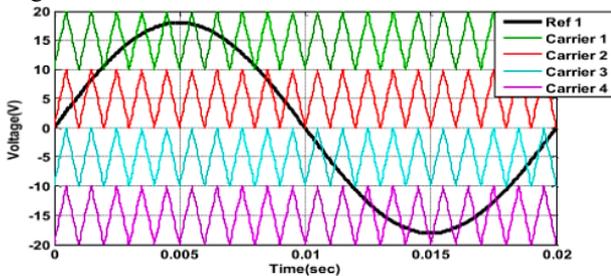

Fig. 5 – PWM level shift control using AMGCN.

Figure 5 shows the PWM level shift using AMGCN. The output voltage and current are controlled by the α, the switches, and are adjusted using AMGCN. Training is performed using simulation data to obtain the optimal management of the bidirectional energy flow in the charging system. The duty cycle is sent to the gate driver circuit, which is

the output of AMGCN. The appropriate signals are produced by the gate driver circuit to operate the switches. The PMD has some control over the result V and I to provide the appropriate charging V and I by altering the obligation pattern of the switch
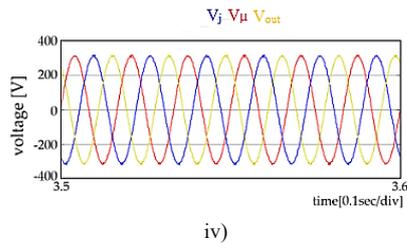

i)

ii)

iii)
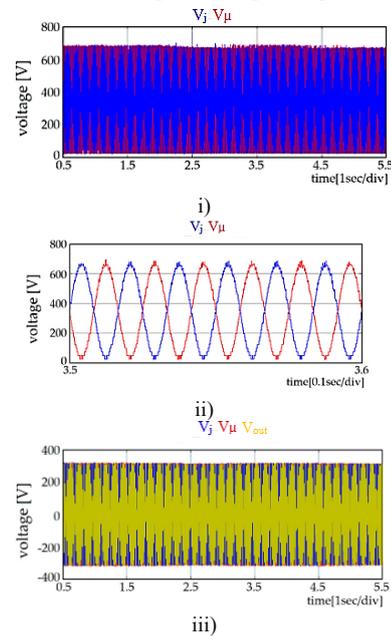
Fig. 6 – Characteristic results of MLDC (i), (ii) voltage waveform over time, (iii), (iv) Voltage response of the system over time.

The findings of the suggested staggered MLDC converter are displayed in Fig. 6. The arm voltages are dealt with in Fig. (i) and (ii), where (ii) provides a more comprehensive view of (i) to clearly display the voltage waveforms. The pole voltage is similarly shown in subfigures (iii) and (iv), where (iv) is an enlarged version of (iii). These charts were produced by simulation with MATLAB Simulink and the suggested simulation circuit.

Hardware implementation:

Figure 7 represents the hardware implementation of the proposed. It consists of various components to ensure efficient power management and control. A DC-DC converter is used to regulate the supply voltage and to ensure stable operation. Measurement tools such as an oscilloscope (Keysight Infinii Vision DSOX1202A, Digital), digital multimeter, and clamp meter (AC/DC, High current range) are employed to monitor voltage, current, and waveform characteristics during testing. The entire system is tested using a load tester to ensure reliability.
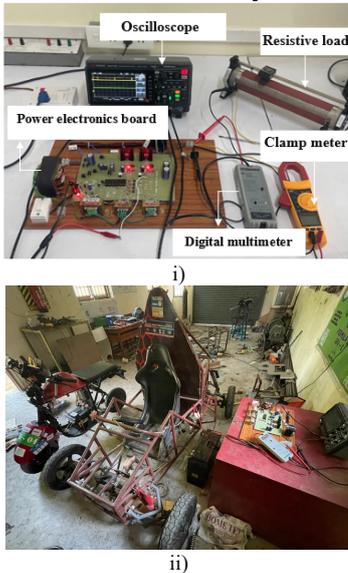

Fig. 7 – Hardware implementation of the proposed MEPO-MGN^2 i) power system testing ii) power management system setup.

4.1 COMPARATIVE ANALYSIS:

The performance of the suggested MLDC converter is contrasted in this section with that of the current converters, such as MMC, MMDC, and MBTR. All comparative results in the manuscript are obtained under identical electrical and operating conditions, and the reported improvements are supported by numerical ripple, efficiency, computational, and transient response metrics.

Figure 8 demonstrated that, for higher input voltages, the proposed converter (MLDC) design was able to produce reduced current ripple values when compared to the existing converter such as MMC, MMDC, and MBTR, respectively. MMC,

MMDC, MBTR, and MLDC (pro) produce approximately 4.0 A, 6.2 A, 5.0 A, and 3.5 A ripple, respectively, whereas at the tenth point these reduce to about 1.4 A (MMC), 2.8 A (MMDC), 2.0 A (MBTR), and only 0.8 A for the proposed MLDC.
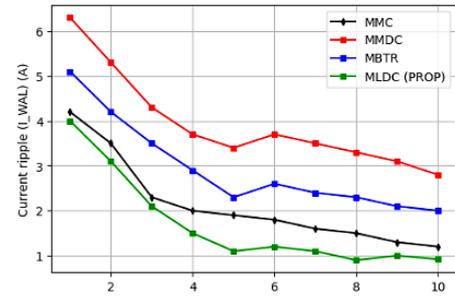

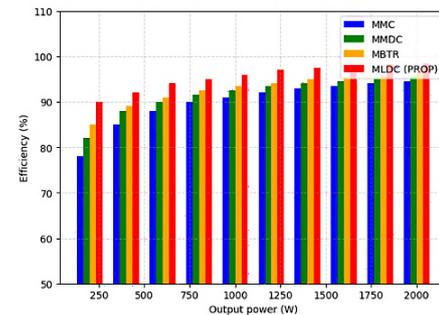Fig. 8 – Current ripple result comparison of existing and proposed converter.

Fig. 9 – Efficiency comparison for different DC-DC converters

Figure 9 represents the efficacy comparison of the proposed and existing converters. The efficiency bar chart shows that the proposed MLDC consistently achieves the highest efficiency across the entire output power range from 250 W to 2000 W. At 250 W, MMC, MMDC, MBTR, and MLDC exhibit approximately 78%, 82%, 85%, and 89% efficiency, respectively, indicating an initial gain of about 7% over MBTR and nearly 11% over MMC. At 1000 W, the efficiencies rise to roughly 91% (MMC), 93% (MMDC), 94% (MBTR), and 96% (MLDC), meaning the proposed MLDC is about 2–5% more efficient than the existing converters. At the rated power of 2000 W, MLDC reaches about 98.5%, whereas MBTR, MMDC, and MMC are around 95%, 94%, and 93%, respectively, giving the proposed design a 3.5–5.5% absolute efficiency advantage and confirming that it delivers superior energy conversion performance, especially under high-load fast-charging conditions.

Table 2

Computational overhead analysis of the proposed MEPO-MGN2 method.

Method	Training Time (s)	Inference Time (s)	Memory Requirement (MB)
Proposed MEPO-MGN^2	0.9	0.7	2.1
LSTM	1.5	1.1	3.5
RNN	2.1	1.9	4.7
CNN	2.8	2.4	7.2
DNN	3.2	2.6	8.5

Table 2 quantitatively shows that the proposed MEPO-MGN^2 method has the lowest computational overhead among all compared learning models. Specifically, MEPO-MGN2 requires only 0.9 s for training and 0.7 s for inference, which is 40% faster than LSTM, 57% faster than RNN, 68% faster than CNN, and 72% faster than DNN in terms of training time. Similarly, its inference time is reduced by 36%, 63%, 71%, and 73%, respectively, compared to LSTM, RNN, CNN, and DNN. In addition, the memory requirement of

MEPO-MGN2 is only 2.1 MB, which is 40% lower than LSTM, 55% lower than RNN, 71% lower than CNN, and 75% lower than DNN. These numerical results clearly demonstrate that MEPO-MGN2 achieves superior computational efficiency while maintaining low memory usage, making it highly suitable for real-time EV charging control applications.

Table 3

Transient response of controllers under different sudden load changes.

Method	Sudden Load Change	Settling Time (ms)	Peak Overshoot (%)	Voltage Dip (%)
MMC	20%	31.8	6.4	5.1
	40%	45.6	9.2	7.8
MMDC	20%	26.4	5.1	4.2
	40%	38.9	7.3	6.0
MBTR	20%	21.2	4.3	3.5
	40%	32.5	6.1	5.0
Proposed MEPO-MGN^2	20%	11.8	1.9	1.4
	40%	17.6	2.8	2.2

Table 3 quantitatively demonstrates that the proposed MEPO-MGN2 controller exhibits superior transient performance under different sudden load changes. For a 20% load increase, MEPO-MGN2 achieves a settling time of only 11.8 ms, which is 44% faster than MBTR (21.2 ms), 55% faster than MMDC (26.4 ms), and 63% faster than MMC (31.8 ms). Its peak overshoot of 1.9% is reduced by 56%, 63%, and 70% compared to MBTR, MMDC, and MMC, respectively, while the voltage dip is limited to 1.4%, far lower than the 3.5–5.1% range of conventional controllers. Under a more severe 40% load disturbance, MEPO-MGN2 still settles within 17.6 ms, which is 46% faster than MBTR, 55% faster than MMDC, and 61% faster than MMC, while maintaining a low overshoot of 2.8% and voltage dip of 2.2%, compared to up to 9.2% overshoot and 7.8% voltage dip in MMC. These numerical results confirm that MEPO-MGN2 provides faster recovery, better damping, and stronger robustness under dynamic load variations than all benchmark controllers.

5. CONCLUSION

In this research, an MLDC converter using a modified Emperor Penguin Optimized multi-graph neural network (MEPO-MGN^2) has been proposed. The power delivered by the grid is changed to DC by means AC-DC converter. This DC voltage is then processed by an MLDC converter, allowing efficient power conversion and bidirectional energy flow, meaning the system can both charge and discharge energy as needed. The proposed method utilizes an Attention Multi-Graph Convolution Network (AMGCN) for the optimal prediction of the duty cycle, and MEPO optimization is employed to tune the parameters of the MLDC converter. Finally, personal mobility devices are charged with a well-regulated DC output voltage. The MEPO-MGN^2 technique thus reduces the charging ripple current to a minimal value, thereby increasing the efficiency. The efficacy of the proposed method is 98.5%, which surpasses the other existing converter techniques. It shows an efficiency improvement of around 18-22% and ripple current average reduction from 16.1% to 47.5%, which is very high when compared to the existing converters. Future research in EV charging stations will focus on improving efficiency and reducing carbon footprints by integrating EV fleets, wireless charging, and WBG-based high-power converters.

REFERENCES

1. Z.M. Ali, M. Calasan, F.H. Gandoman, F. Jurado, S.H.A. Aleem, *Review of battery reliability in electric vehicle and E-mobility applications*, Ain Shams Engineering Journal, **15**, *2*, 102442 (2024).
2. Y. Cao, J. Cui, S. Liu, X. Li, Q. Zhou, C. Hu, Y. Zhuang, Z. Liu, *A holistic review on e-mobility service optimization: challenges, recent progress, and future directions*, IEEE Transactions on Transportation Electrification, **10**, *2*, pp. 3712–3741 (2023).
3. L. Prause, K. Dietz, *Just mobility futures: challenges for e-mobility transitions from a global perspective*, Futures, **141**, 102987 (2022).
4. M. Nigro, M. Ferrara, R. De Vincentis, C. Liberto, G. Valenti, *Data-driven approaches for sustainable development of E-mobility in urban areas*, Energies, **14**, *13*, 3949 (2021).
5. L. Devarajan, S. Chellathurai, *Aquila optimized nonlinear control for DC-DC boost converter with constant power load*, Rev. Roum. Sci. Techn. – Électrotechn. et Énerg., **69**, *4*, pp. 419–424 (2024).
6. G. Isha, P. Jagatheeswari, J. Gnana Malar, *An elitist Harris Hawks optimized voltage stability enhancement in radial distribution system*, Journal of Electrical Engineering & Technology, **18**, pp. 2683–2693 (2023).
7. S. Valedsaravi, A. El Aroudi, L. Martínez-Salamero, *Review of solid-state transformer applications on electric vehicle DC ultra-fast charging station*, Energies, **15**, *15*, 5602 (2022).
8. D. Savio Abraham, R. Verma, L. Kanagaraj, S.R. Giri Thulasi Raman, N. Rajamanickam, B. Chokkalingam, K. Marimuthu Sekar, L. Mihet-Popa, *Electric vehicles charging stations' architectures, criteria, power converters, and control strategies in microgrids*, Electronics, **10**, *16*, 1895 (2021).
9. M. Kuppusamy, N. Muthukumaran, R. Raja Lakshmi, R. Sangno, *Multi-term islanding protection and load priority-based optimal shedding framework for maintaining voltage stability and loadability in microgrid systems*, Electrical Engineering (2023).
10. G. Rajendran, C.A. Vaithilingam, N. Misron, K. Naidu, M.R. Ahmed, *A comprehensive review on system architecture and international standards for electric vehicle charging stations*, Journal of Energy Storage, **42**, 103099 (2021).
11. J.H. Lee, S.J. Park, S.K. Lim, *Improvement of multilevel DC/DC converter for e-mobility charging station*, Electronics, **9**, *12*, 2037 (2020).
12. G. Sha, Q. Duan, W. Sheng, C. Ma, C. Zhao, Y. Zhang, J. Tian, *Research on multi-port DC-DC converter based on modular multilevel converter and cascaded H-bridges for MVDC applications*, IEEE Access, **9**, pp. 95006–95022 (2021).
13. X. Han, H. Wen, *Analysis and design of modular multi-level DC/DC converter*, 2021 IEEE 16th Conference on Industrial Electronics and Applications (ICIEA), pp. 649–654 (2021).
14. S. Sarkar, A. Das, *An isolated single input-multiple output DC–DC modular multilevel converter for fast electric vehicle charging*, IEEE Journal of Emerging and Selected Topics in Industrial Electronics, **4**, *1*, pp. 178–187 (2022).
15. S.K. Dube, R. Nair, V. Beaston, P. Das, *A multilevel three-phase integrated AC-DC bidirectional resonant converter for BESS*, IEEE Journal of Emerging and Selected Topics in Power Electronics (2023).
16. Y. Huang, S. Lin, H. Mo, *Three-level bidirectional DC/DC intelligent control technology for photovoltaic charging station of electric vehicle combined with SVPWM algorithm*, IEEE Access (2023).
17. K.B. Ray, R. Kumar, *SOC-based fast and stable charging control using multilevel DC-DC buck converter for EVs*, IETE Journal of Research, **70**, *2*, pp. 2178–2192 (2024).
18. G. Jothimani, K. Mahalingam, P. Karuppasamy, *A double switch integrated high-gain quadratic boost converter for electric vehicle applications*, Rev. Roum. Sci. Techn. – Électrotechn. et Énerg., **70**, *4*, pp. 495–500 (2025).
19. M. Duraisamy, *Analysis and experimental validation of a non-isolated DC-DC SEPIC-modified CUK combined converter*, Rev. Roum. Sci. Techn. – Électrotechn. et Énerg., **70**, *3*, pp. 367–372 (2025).